Spin Dynamics in a Superconductor-Ferromagnet Proximity System

C. Bell,[1] S. Milikisyants,[2] M. Huber,[2] and J. Aarts[3]

[1]*Magnetic and Superconducting Materials Group, Kamerlingh Onnes Laboratorium, Universiteit Leiden, The Netherlands*
[2]*Molecular Nano-Optics and Spins Group, Huygens Laboratory, Universiteit Leiden, The Netherlands*
[3]*Magnetic and Superconducting Materials Group, Kamerlingh Onnes Laboratory, Universiteit Leiden, The Netherlands*

(Received 3 March 2007; published 1 February 2008)

The ferromagnetic resonance of thin sputtered $Ni_{80}Fe_{20}$ films grown on Nb is measured. By varying the temperature and the thickness of the Nb the role of the superconductivity on the whole ferromagnetic layer in these heterostructures is explored. The change in the spin transport properties below the superconducting transition of the Nb is found to manifest itself in the $Ni_{80}Fe_{20}$ layer by a sharpening in the resonance of the ferromagnet, or a decrease in the effective Gilbert damping coefficient, showing that the superconductivity affects the macrospin of the ferromagnetic layer. We interpret this in terms of the spin-pumping model.

DOI: 10.1103/PhysRevLett.100.047002 PACS numbers: 74.45.+c, 72.25.Mk, 73.40.−c, 76.50.+g

Most of the experiments in the field of superconductor (S)-ferromagnet (F) hybrids rely on measuring their electrical transport characteristics. In S/F/S Josephson junctions the measured quantity is mainly the supercurrent, which is, for instance, used to show the existence of π junctions (where the phase of the order parameter undergoes a change of phase by π) [1]. More recently, experiments involving a half-metallic ferromagnet found the supercurrent in that case to be long ranged, possibly due to the occurrence of spin-triplet superconductivity [2]. Also in F/S/F structures, spin injection in superconductors is mostly measured and analyzed by following the changes in electrical resistance of the device [3].

For questions involving spin transport as well as for studying the nature of the superconducting correlations inside the ferromagnet, it would be advantageous to have a method which measures changes of the F layer properties as a consequence of the superconductivity. In hybrids of normal metals (N) and ferromagnets, similar questions are currently addressed by ferromagnetic resonance (FMR) experiments in the microwave regime, which study the dynamic behavior of the precessing ferromagnetic spin of the F layer in good electrical contact with an N layer. The decay of the precessing magnetization $\mathbf{m}$, and therefore the power absorption, can be written in terms of the Landau-Lifshitz-Gilbert equation as

$$\partial_t \mathbf{m} = -\gamma \mathbf{m} \times \mathbf{H}_{\text{eff}} + \alpha \mathbf{m} \times \partial_t \mathbf{m}, \quad (1)$$

where γ is the gyromagnetic ratio, $\mathbf{H}_{\text{eff}}$ is an effective magnetic field, and α is the Gilbert constant which controls the damping. This parameter is often further parametrized as $G = \alpha\gamma M_s$, with M_s the saturation magnetization of the F layer. Experiments usually record the derivative of the power absorption upon varying the applied magnetic field, and the resulting line consists of a positive lobe, a zero crossing, and a negative lobe. It can be characterized by the field value H_0 of the crossing (the resonance field), and the linewidth ΔH_{pp} (the field separation between the positive and negative peaks). There are different contributions to the linewidth, which can yield either homogeneous (ΔH_{hom}) or inhomogeneous broadening (ΔH_{inhom}). Sample imperfections, resulting in variations of, e.g., saturation magnetization and anisotropy fields, yield inhomogeneous broadening assumed to be independent of the measurement frequency ω. Gilbert damping as formulated in Eq. (1) results in a homogeneous broadening which is proportional to ω. The linewidth ΔH_{pp} is therefore often expressed as [4]

$$\Delta H_{\text{pp}} = \Delta H_{\text{inhom}} + \Delta H_{\text{hom}} = \Delta H_{\text{inhom}} + \frac{2G\omega}{\sqrt{3}\gamma^2 M_s}. \quad (2)$$

In the F/N case, the homogeneous damping is caused in part by the emission of spin-polarized electrons in a direction perpendicular to the interface, which leads to the spin-pumping or spin battery effect. Hence the properties of the nearby metals in a heterostructure play a critical role in determining the FMR line shape, as has been reviewed in detail by Tserkovnyak *et al.* [5]. Few FMR experiments have been reported as yet for F/S systems. In Fe/Nb bilayers the angular dependence of the resonance field was studied. The analysis indicated a slight decrease of the effective magnetization of the Fe layer below T_c [6]. Another study was reported on bulk $RuSr_2GdCu_2O_8$ [7], but here superconductivity and ferromagnetism are intrinsically mixed, which gives rise to a different situation. On the other hand, there are by now several theoretical predictions concerning such experiments. In ferromagnetic superconductors the symmetry of the order parameter might be identifiable [8,9], while S/F/S junctions are to show unconventional spin wave dynamics [10], or conductance resonances in the presence of precessing spins [11]. Here we address the first basic question in this field, namely, the effect of the proximity of a superconductor (Nb) on the FMR linewidth of a strong ferromagnet ($Ni_{80}Fe_{20}$, Permalloy, Py) and find significant changes in the homogeneous broadening. The results imply that the entire

magnetic layer is affected rather than the small distance of the superconducting coherence length in the magnet.

Our samples are grown on 0.5 mm thick Suprasil® 2 quartz (lateral dimensions $\sim$3 mm $\times$ 5 mm) by dc magnetron sputtering at room temperature, in a vacuum system with a base pressure $<2 \times 10^{-9}$ mbar. Deposition rates were $\sim$0.12 nm/s for the Nb and $\sim$0.14 nm/s for the Py, as calibrated from low angle x-ray reflectivity. We focus on three different samples. Sample A consists of q/Nb(70)/Py(5), with q the quartz substrate and the numerals giving the layer thickness in nm; sample B is q/Nb(9)/Py(5), and sample C is q/Nb(70)/Py(2)/Nb(5). The critical temperature $T_c \sim 8.2$ K of sample A was measured in an in-plane magnetic field of $\mu_0 H = 100$ mT. The transition width was <30 mK, and the resistance ratio was $R(300\ \mathrm{K})/R(10\ \mathrm{K}) = 3.1$. For sample B the 9 nm thick Nb layer is below the critical thickness of the S layer and does not superconduct in the range of temperatures presented. Sample B thus serves as a reference with similar interface characteristics, but no superconductivity. Both samples have an unprotectedF layer; sample C has a thinner Py layer as well as a nonsuperconducting (Nb) protection cap.

Because of stray magnetic fields in the sputtering chamber, the Py possesses an in-plane uniaxial induced anisotropy, giving a coercive field $\mu_0 H_C^{\mathrm{easy}} = 3.5$ mT for sample A ($T = 10$ K), with $H_C^{\mathrm{easy}} \sim 0.8 \times H_C^{\mathrm{hard}}$. All data presented are measured with the applied field nominally along the easy axis. The FMR measurements were made in a Bruker ElexSys E680 X-band electron paramagnetic resonance system operating at 9.5 GHz, equipped with a rectangular TE_{102} cavity and a liquid helium continuous flow cryostat. The input power was nominally 220 mW, attenuated before the resonance cavity by a factor of 10^4 (40 dB). The dc magnetic field was applied with a modulation of $\mu_0 H = 0.5$ mT at 100 kHz. The samples were secured with Teflon tape onto a quartz rod mounted vertically on a goniometer to allow control of the film normal direction with respect to the applied field: this was optimized at room temperature to be 90° $\pm$ 2° by minimizing the center field of the FMR. Some typical FMR spectra taken for sample A, and after subtracting a small linear background, are shown in Fig. 1 above and below the superconducting transition. The line shape is close to the derivative of a Lorentzian line, with the ratio of the amplitudes of the lobes around 0.8. This asymmetry has been observed in many other systems [12] and is associated with the polycrystalline nature of the samples, and variations of saturation magnetization and anisotropy fields over the sample. In the figure we also define the two parameters used to quantify changes in the resonance conditions, the zero-crossing field H_0 and the linewidth ΔH_{pp} (the field separation between the peak and dip position). Figure 2 shows the central result of our Letter. Here we plot ΔH_{pp} versus temperature T around T_c for all three samples. The first thing to note is that the superconducting samples (A and C) both show a significant nonmonotonic decrease in linewidth, of the order of 20% when cooling through T_c. The nonsuperconducting sample (B) does not show such an anomaly. This indicates a strong *decrease* of the damping experienced by the precessing magnetization in the F layer when the adjacent S layer becomes superconducting. Before discussing this further we comment on some details of the data.

First, we demonstrate that the change in ΔH_{pp} is actually representative of a change in the full absorption line shape. This is not obvious from Fig. 2, because both the peak heights and the zero crossing are changing as a function of temperature. In Fig. 3 we plot line shapes of the (superconducting) sample A and the (normal) sample B at temperatures around the jump in ΔH_{pp} observed in sample A. The intensity is normalized by the minimum value in the negative lobe, while the applied field is scaled on the resonance field H_0. This latter is appropriate for the homogeneous component of the linewidth, because of the proportionality to ω (and therefore to H_0) mentioned above.

It is clear from Fig. 3 that the jump in ΔH_{pp} observed for sample A is reflected in a sharpening up of the complete

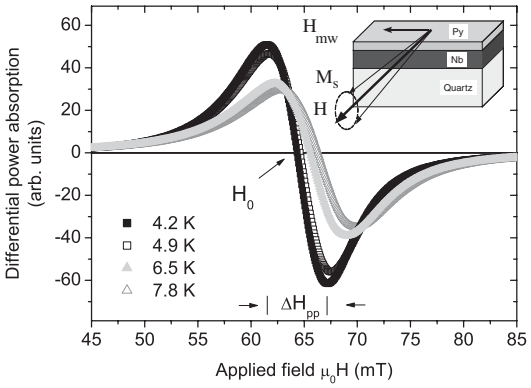

FIG. 1. FMR spectra for sample A taken around T_c. ΔH_{pp} and H_0 for the $T = 4.2$ K spectrum are labeled. The inset shows the directions of the static field H, the microwave field H_{mw}, the saturation magnetization M_s, and the precession of M_s due to the microwave field.

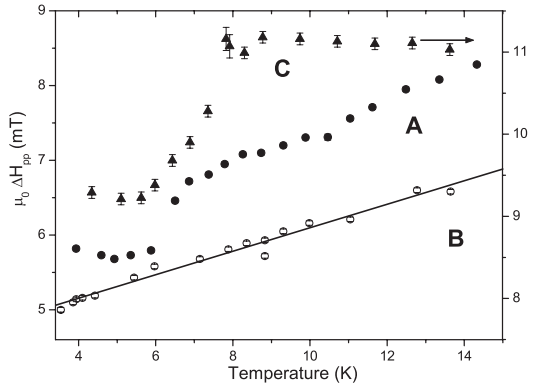

FIG. 2. Variation of ΔH_{pp} with temperature T for samples A (sc), B (non-sc), and C (sc) for $T < 15$ K. Note the different scale for sample C. The line is a guide to the eye.

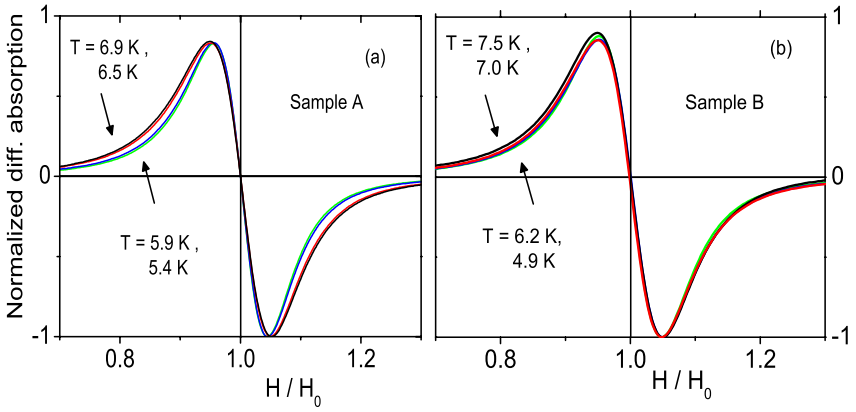

FIG. 3 (color online). Differential absorption, normalized on the value of the negative lobe versus applied field H, scaled on the resonance field H_0 for (a) sample A (sc) at temperatures 6.9 K, 6.5 K, 5.9 K, and 5.4 K (from the top curve to the bottom curve); (b) sample B (normal) at temperatures 7.5 K, 7.0 K, 6.2 K, and 4.9 K (from the top curve to the bottom curve).

line, visible in a range of 30% around H_0, and also that this sharpening up is homogeneous in nature. The nonsuperconducting sample B does not show this sudden sharpening.

The values of ΔH_{pp} in the normal state are different for all samples. The larger linewidth in sample C is simply due to the much smaller thickness of the F layer; the different values for samples A and B are caused, we believe, by the thicker Nb layer present in sample A and the influence of that layer on the spin-pumping effect, as will be discussed below. Furthermore, still in the normal state, ΔH_{pp} for samples A and B shows a clear temperature dependence which is absent in sample C. This is caused by the difference between the capped and uncapped Py. To illustrate this point more clearly we show the temperature dependence over a wider range in Fig. 4(a). For the uncapped samples, ΔH_{pp} actually goes through a maximum around 40 K, while the linewidth of the uncapped sample is only weakly temperature dependent. This is in agreement with earlier work on single Py films, where similar variations were found for films with a native oxide or with a magnetic (NiO) cap, while no temperature dependence was observed for Cu-capped Py [13]. The native oxide apparently acts as a different magnetic system which influences the Py.

This can also be seen in the temperature dependence of H_0, Fig. 4(b). For the uncapped samples H_0 shows a decrease below 50 K, while H_0 for sample C is again changing only slightly in this regime. Around T_c, no significant anomalies are found in the behavior of H_0 [inset of Fig. 4(b)]; sample A appears to show a slight downturn, and sample C an even smaller upward deviation. The substantial decrease in linewidth for both samples is thus not due to variations in the effective field experienced.

Returning to our main observation of the change in FMR linewidth at T_c, we wish to argue that this is due to suppression of the spin-sinking mechanism which is provided by the normal layer, when this layer becomes superconducting. For this, we first refer to a set of studies by Mizukami *et al.* [14] who showed that the linewidth and the Gilbert damping coefficient G slightly increased when a Cu layer of increasing thickness was deposited on a thin Py film, whereas the linewidth became much larger when Pt was deposited instead, and that this width decreased again when a Cu layer was inserted between the Py and the Pt. The basic explanation for these observations (see [5]) is that the precessing moment drives spins into the normal metal, which leads to increased damping if the spin angular momentum is removed from the system by a spin scattering event. When the metal is dirty the diffusive motion increases the probability that, due to spin flip processes, electrons with opposite spin are scattered back into the magnet, which leads to stronger damping, especially when the normal metal is characterized by strong spin-orbit scattering. This explains both the small increase upon Cu deposition and the much larger increase with a Pt layer. Needless to say, when a Cu layer is placed between the Py and the Pt, the damping will decrease again with increasing thickness of the Cu layer.

In this model for spin pumping, a smaller Gilbert damping in the superconducting state (well below T_c) can be

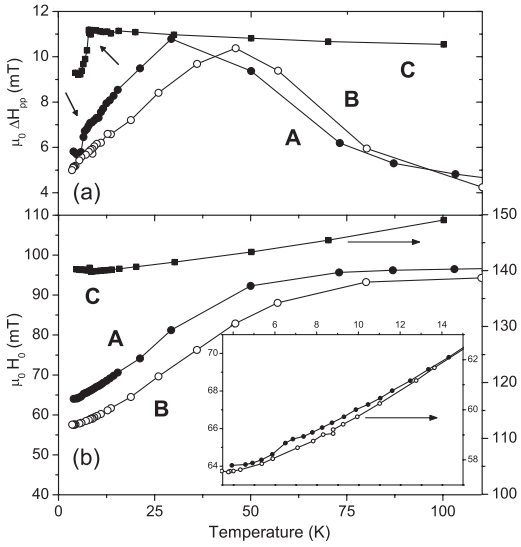

FIG. 4. (a) Variation of ΔH_{pp} with temperature T for samples A, B, and C. The arrows denote the strong decrease of ΔH_{pp} at T_c for samples A and C. (b) Variation of H_0 with T for the same samples. Note the different scale for sample C. Lines are a guide. Inset: H_0 data for A and B below 15 K.

understood since spin transport is forbidden in the superconductor. Electrons ejected from the ferromagnet have energies well below the superconducting gap of Nb (1.5 meV at $T = 0$ K) and therefore cannot enter the superconductor as quasiparticles. The other mechanism to enter is through Andreev reflections (AR), in which a spin-up electron and a spin-down electron combine into a Cooper pair. In this case, no net spin or magnetization is removed from the system, and the damping will be smaller than in the normal state. This needs two further comments. One is that, on the superconducting side of the interface, the gap is almost fully suppressed by the presence of the ferromagnet and only recovers at a distance from the interface given by roughly twice the (dirty limit) coherence length ξ_S. In this region of suppressed gap electrons move diffusively, with some probability of spin-flipping and backscattering. So, if, for instance, strong spin-orbit scattering is present, characterized by a small value of the spin flip length λ_{sf} in the normal state, that will diminish the effect of AR. For Nb this will not be an important effect since $\xi_S \approx 10$ nm is sufficiently smaller than $\lambda_{\mathrm{sf}} \approx 50$ nm [15]. The other comment is that the spin subbands of the ferromagnet are not equally populated, which means that part of the electrons undergo normal reflection at the S/F interface rather than Andreev reflection [16,17]. The effect is the same, since also the normal reflections leave the magnetization unchanged, with one subtle difference: the normal reflections take place close to interface rather than within a distance ξ_s of the interface, making the F layer even more immune for the possibilities of spin flips in the region of suppressed order parameter.

With respect to the magnitude of the variation in ΔH_{pp} we observe, it should be clear now that the difference in damping between the normal state and the superconducting state is largest when the metal acts as an efficient "spin sink" in the normal state. This efficiency is measured by the parameter $\epsilon = \tau_e/\tau_{\mathrm{sf}}$, the ratio between the momentum scattering time τ_e, and the spin flip scattering time τ_{sf}, which can also be written in terms of the respective lengths as $\frac{1}{3}(\ell/\ell_{\mathrm{sf}})^2$. For the Nb films with $\ell \approx 5$ nm, $\epsilon = 0.005$, which is a bit low compared to $\epsilon \geq 0.01$ required for efficient spin sinking [5]. A quantitative theoretical treatment of this problem, yielding the correct order of magnitude for ΔH_{pp}, is forthcoming [18]. Incidentally, the above picture also explains the difference between ΔH_{pp} for samples A and B in the normal state: the thicker Nb layer of sample A is slightly more effective in backscattering opposite spins.

To summarize, we have shown that a superconductor in good metallic contact with a ferromagnet influences the dynamics of the whole ferromagnetic layer by decreasing the spin sink efficiency, leading to a decreased Gilbert damping of the FMR. The decrease in the damping of the F layer is highly relevant for S/F hybrid devices with strong ferromagnets [19,20] at high frequencies, in, for example, possible coupling between the FMR and the ac Josephson effect [21]. These issues have not been addressed so far, and we want to stress the potential usefulness of the FMR technique. Moreover, an interesting question is if any additional effects can be observed due to the inhomogeneous induced superconducting state in the Py, which penetrates over 1–1.5 nm [19], meaning that a significant fraction of the Py in our experiments experiences induced superconductivity. Also studies with F/S/F trilayers or a S/half metal system would be interesting, since superconducting triplet components [22] are expected to contribute to the FMR damping in a different way [8].

We want to thank J. Schmidt, G. E. W. Bauer, A. Brataas, J. P. Morten, and A. A. Golubov for discussions. This work is part of the research programme of the "Stichting voor Fundamenteel Onderzoek der Materie (FOM)," which is financially supported by the "Nederlandse Organisatie voor Wetenschappelijk Onderzoek (NWO)."

[1] A. I. Buzdin, Rev. Mod. Phys. **77**, 935 (2005).
[2] R. S. Keizer *et al.*, Nature (London) **439**, 825 (2006).
[3] J. Y. Gu *et al.*, Phys. Rev. B **66**, 140507(R) (2002).
[4] W. Platow *et al.*, Phys. Rev. B **58**, 5611 (1998).
[5] Y. Tserkovnyak *et al.*, Rev. Mod. Phys. **77**, 1375 (2005).
[6] Th. Mühge *et al.*, Physica (Amsterdam) **296C**, 325 (1998).
[7] A. Fainstein *et al.*, Phys. Rev. B **60**, R12 597 (1999).
[8] A. Brataas and Y. Tserkovnyak, Phys. Rev. Lett. **93**, 087201 (2004).
[9] V. Braude, Phys. Rev. B **74**, 054515 (2006).
[10] Z. Nussinov *et al.*, Phys. Rev. B **71**, 214520 (2005).
[11] Y.-M. Shi *et al.*, Europhys. Lett. **73**, 941 (2006).
[12] C. Chappert *et al.*, Phys. Rev. B **34**, 3192 (1986).
[13] P. Lubitz *et al.*, J. Appl. Phys. **83**, 6819 (1998).
[14] S. Mizukami, Y. Ando, and T. Miyazaki, Phys. Rev. B **66**, 104413 (2002); J. Magn. Magn. Mater. **226–230**, 1640 (2001); Jpn. J. Appl. Phys. **40**, 580 (2001).
[15] T. Yamashita *et al.*, Phys. Rev. B **67**, 094515 (2003).
[16] F. J. Jedema *et al.*, Phys. Rev. B **60**, 16 549 (1999).
[17] M. J. M. de Jong and C. W. J. Beenakker, Phys. Rev. Lett. **74**, 1657 (1995).
[18] J. P. Morten (private communication).
[19] J. W. A. Robinson *et al.*, Phys. Rev. Lett. **97**, 177003 (2006).
[20] F. Born *et al.*, Phys. Rev. B **74**, 140501(R) (2006).
[21] X. Waintal and P. W. Brouwer, Phys. Rev. B **65**, 054407 (2002).
[22] Y. V. Fominov, A. A. Golubov, and M. Y. Kupriyanov, JETP Lett. **77**, 510 (2003).